Chemistry & Biology
Article

Membrane-Permeant Phosphoinositide Derivatives as Modulators of Growth Factor Signaling and Neurite Outgrowth

Vibor Laketa,[1,3] Sirus Zarbakhsh,[1,3] Eva Morbier,[2] Devaraj Subramanian,[1] Carlo Dinkel,[1] Justin Brumbaugh,[1] Pascale Zimmermann,[2] Rainer Pepperkok,[1] and Carsten Schultz[1,*]
[1]Cell Biology and Cell Biophysics Unit, European Molecular Biology Laboratory, Meyerhofstraße 1, 69117 Heidelberg, Germany
[2]Department of Human Genetics, K.U. Leuven, B-3000 Leuven, Belgium
[3]These authors contributed equally to this work
*Correspondence: schultz@embl.de
DOI 10.1016/j.chembiol.2009.10.005

SUMMARY

Phosphoinositides are important signaling molecules that govern a large number of cellular processes such as proliferation, differentiation, membrane remodeling, and survival. Here we introduce a fully synthetic membrane-permeant derivative of a novel, easily accessible, and very potent phosphatidylinositol 3,4,5-trisphosphate [PtdIns(3,4,5)P_3] mimic: phosphatidylinositol 3,4,5,6-tetrakisphosphate [PtdIns(3,4,5,6)P_4]. The membrane-permeant PtdIns(3,4,5,6)P_4 derivative activated pathways downstream of phosphatidylinositol 3-kinase (PI3K), including protein kinase B, p70S6K, mitogen-activated protein kinase, and protein kinase C, more potently than similar membrane-permeant PtdIns(3,4,5)P_3 and PtdIns(3,4)P_2 derivatives in the absence of receptor stimulation. In addition, we demonstrate that treatment of PC12 cells with the membrane-permeant PtdIns(3,4)P_2, PtdIns(3,4,5)P_3, and PtdIns(3,4,5,6)P_4 derivatives increases the number of neurites per cell in the presence of NGF. This work establishes membrane-permeant phosphoinositides as powerful tools to study PI3K signaling and directly demonstrates that 3-phosphorylated phosphoinositides are instrumental for neurite initiation.

INTRODUCTION

Intracellular signaling mediated by growth factors activate various phosphoinositide 3-kinase (PI3K) isoforms (Cantley, 2002), which phosphorylate phosphoinositides like phosphatidylinositol 4,5-bisphosphate [PtdIns(4,5)P_2] at the 3-hydroxy group of the inositol ring, giving rise to phospholipids such as phosphatidylinositol 3,4,5-trisphosphate [PtdIns(3,4,5)P_3; **2**] and phosphatidylinositol 3,4-bisphosphate [PtdIns(3,4)P_2]. PtdIns(3,4,5)P_3 and PtdIns(3,4)P_2 are recognized as second messengers that govern many downstream events by activating target protein kinases such as PDK1, which subsequently phosphorylate various signaling proteins including p70S6K, protein kinase B (also known as Akt), and protein kinase C (PKC) (Figure 1A) (Cantley, 2002).

So far an effective approach to manipulate phosphoinositide levels for investigating signaling is to overexpress or knock down phosphoinositide-forming or metabolizing enzymes. However, these methods require hours or days to develop an effect and often the response is wiped out by a compensation mechanism. Therefore, there is a necessity for methods that alter phosphoinositide levels within minutes, resulting in a better control of the experiment, a more immediate onset of the signal, and therefore more physiological mimicking of the growth factor signaling. One way to alter intracellular phosphoinositide levels would be to modulate the activity of engineered phosphoinositide metabolizing enzymes with a "chemical dimerizer" such as rapamycin (Suh et al., 2006). Another, more direct, possibility uses synthetic membrane-permeant derivatives of these phospholipids (Dinkel et al., 2001; Jiang et al., 1998). This involves masking the charged phosphate groups by bioactivatable acetoxymethyl esters (AM esters). The uncharged AM esters are sufficiently stable outside cells to be applied in regular buffers. Once the derivatives enter cells, enzymatic cleavage of the bioactivatable esters leads to unmasking of phosphates and the reconstitution of negative charges and biological function (Schultz, 2003). In addition, butyrates are frequently used to mask the hydroxy groups (Vajanaphanich et al., 1994). Their enzymatic hydrolysis is slower than AM ester hydrolysis (Bartsch et al., 2003), thereby preventing phosphates from scrambling during bioactivation. Upon addition to cells, the lipophilic derivatives pass the plasma membrane by diffusion (Figure 1B). Once reaching the cytosol, endogenous unspecific carboxyhydrolases are expected to first remove the AM esters and subsequently the butyrates, thereby releasing the phosphoinositide of interest or an active metabolite. We previously applied the AM ester technique to show that a membrane-permeant derivative of PtdIns(3,4,5)P_3 (**5**; Figure 1C), but not PtdIns(3,4)P_2 (**7**; Figure 1C), reduced chloride secretion of epithelial cells (Dinkel et al., 2001). An alternative to bioactivatable masking groups are cationic polyanions for permitting phospholipid entrance to living cells (Ozaki et al., 2000).

The total synthesis of membrane-permeant PtdIns(3,4,5)P_3 (**5**) and PtdIns(3,4)P_2 (**7**) derivatives required an enormous synthetic effort (Dinkel et al., 2001). A derivative with an additional

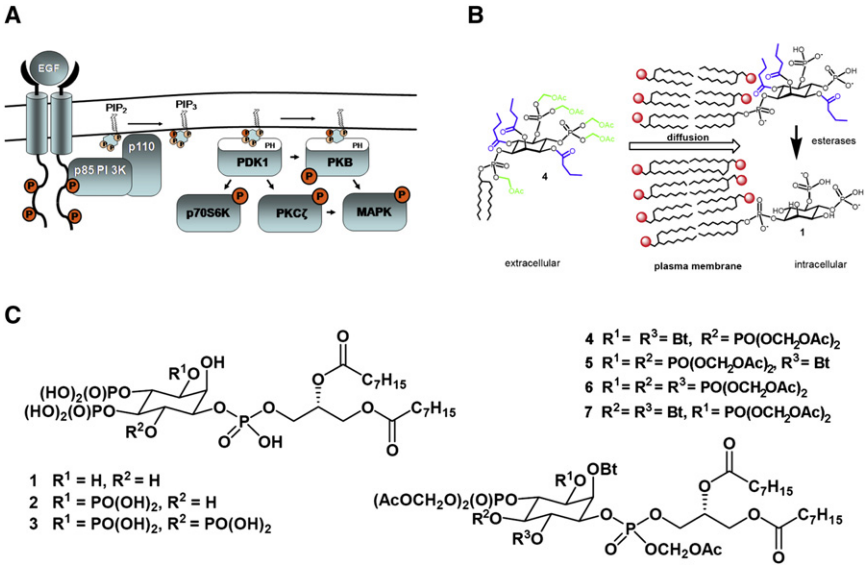

Figure 1. Growth Factor Signaling, Membrane-Permeant Phosphoinositide Derivatives, and Their Mode of Cell Delivery

(A) A simplified EGF/PI3K signaling pathway. PIP_2, PtdIns(4,5)P_2; PIP_3, PtdIns(3,4,5)P_3.

(B) Mechanism of membrane-permeant phosphoinositide derivative cell entry and activation. The negatively charged phosphate groups of the phospholipid are masked with enzyme cleavable AM ester groups (green) while hydroxy groups are masked by butyrates (blue). The uncharged molecule diffuses across the plasma membrane. Inside the cell the protecting groups are cleaved by endogenous enzymes and the active compound is liberated.

(C) Phosphoinositides and their membrane-permeant derivatives. The naturally occurring phosphoinositides PtdIns(4,5)P_2 (**1**) and PtdIns(3,4,5)P_3 (**2**), the artificial tetrakisphosphate PtdIns(3,4,5,6)P_4 (**3**), and the respective membrane-permeant derivatives **4** to **6** are shown. A similar derivative of PtdIns(3,4)P_2 (**7**) is also shown. Please note that all lipid moieties have unnatural octanoic acid esters unless stated otherwise. Bt, butyrate; Ac, acetate.

phosphate in the 6 position would be much easier to prepare. Furthermore, very little is known about structure-activity relationships of phosphoinositides, mainly due to a lack of synthetic chemistry efforts and solubility problems of the phosphoinositides in physiologically relevant buffers. To facilitate the preparation of membrane-permeant PtdIns(3,4,5)P_3 (**5**) and PtdIns(3,4)P_2 (**7**) derivatives and to study relationship between phosphoinositide structure and their activity, we extended the masking approach to a previously unknown phosphoinositide, PtdIns(3,4,5,6)P_4 (**3**). We performed a comprehensive biochemical and live cell analysis of membrane-permeant phosphoinositide derivative effects on intracellular signaling pathways downstream of PI3K. This demonstrated that membrane-permeant phosphoinositides are able to stimulate many aspects of PI3K-dependent signaling. Remarkably, PtdIns(3,4,5,6)P_4/AM behaves like a much more potent activator of the PI3K pathway than membrane-permeant PtdIns(3,4)P_2 and PtdIns(3,4,5)P_3 derivatives. In addition, we examined the role of membrane-permeant phosphoinositides in a more complex PI3K-dependent process such as neurite outgrowth, where we show that addition of membrane-permeant PI3K products induces an increase in the number of neurites per cell, indicating their role in neurite initiation.

RESULTS

Synthesis of Membrane-Permeant PtdIns(3,4,5,6)P_4 Derivative

We prepared 2-*O*-butyryl-phosphatidylinositol 3,4,5,6-tetrakisphosphate nonakis(acetoxymethyl) ester (PtdIns(3,4,5,6)P_4/AM, PIP_4/AM, **6**), starting from commercially available enantiomerically pure 1,2-*O*-cyclohexylidene-*myo*-inositol (**8**; Figure 2). Phosphorylation was achieved using standard dibenzyl phosphoramidite chemistry in excellent yield. Deprotection of the ketal under acidic conditions gave the tetrakisphosphate derivative **9**. After regioselective butyrylation of the axial 2-OH group over the 1-OH position (85:15) via formation of an intermediate orthoester, 1,2-di-*O*-octanoyl-*sn*-glycerol 3-(benzyl *N*,*N*-di*iso*propyl)phosphoramidite (**10**) was used to introduce of the lipid moiety. The fully protected PtdIns(3,4,5,6)P_4 derivative **11** was quantitatively deprotected by catalytic hydrogenolysis. The resulting free acid was alkylated to the final nonakis(acetoxymethyl) ester **6** by using 27 equivalents of acetoxymethyl bromide and an equimolar amount of *N*,*N*-di*iso*propylethylamine in acetonitrile. PIP_4/AM (**6**) was purified to homogeneity by preparative HPLC. This synthetic pathway involved only six synthetic steps plus the formation of the lipid phosphoramidite and provides the simplest access to a highly phosphorylated membrane-permeant phosphoinositide derivative known so far. The overall yield from **8** was 19%. In a similar way, a di-*O*-myristylglyceryl derivative was prepared (data not shown).

Phosphoinositide Derivatives Activate Signaling Networks Downstream of PI3K

First, we tested how all membrane-permeant phosphoinositide derivatives affect different aspects of PI3K-dependent intracellular signaling. Mitogen-activated protein kinases (MAPKs) provide a functional signaling "hub" where signaling inputs are amplified and integrated (Cuevas et al., 2007) and thus MAPK phosphorylation levels are a good marker of intracellular signaling activity. Therefore, we first investigated p42/p44 MAPK phosphorylation after treatment with different membrane-permeant phosphoinositide derivatives. All 3-phosphorylated phosphoinositides tested induced p42/p44 MAPK phosphorylation (Figure 3A), while the corresponding membrane-permeant PtdIns(4,5)P_2 derivative was inactive (see Figure S1A available online). Remarkably, the membrane-permeant PtdIns(3,4,5)P_3 (PIP_3/AM, **5**) and PtdIns(3,4)P_2 (PI(3,4)P_2/AM) derivatives were significantly less potent than the PtdIns(3,4,5,6)P_4 derivative (PIP_4/AM, **6**) (Figure 3A and see the quantification in Figure S1B). The induction of p42/p44 MAPK phosphorylation was unchanged in the presence of PI3K inhibitor wortmannin

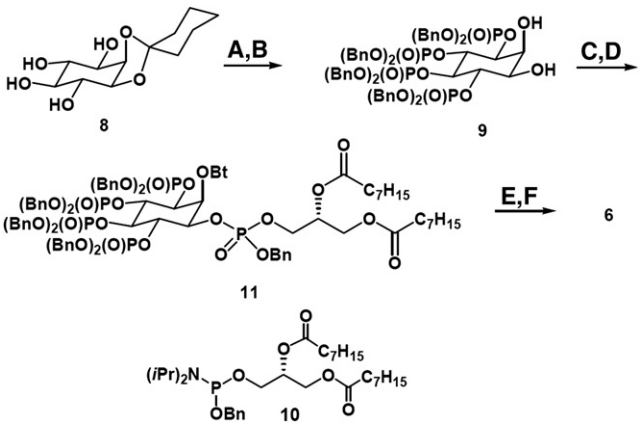

Figure 2. Synthesis of the Membrane-Permeant Phosphoinositide PIP_4/AM (6)

(A) $(BnO)_2PNiPr_2$, DCI, MeCN, 1d, then −40°C, CH_3CO_3H, 84%.
(B) TFA/$CHCl_3$, 78%.
(C) $C_3H_7C(OMe)_3$, PPTS-resin, CH_2Cl_2, H_2O, 80%.
(D) **10**, DCI, DCM, then −40°C, CH_3CO_3H, 80%.
(E) Pd/C, H_2, 99%.
(F) $AcOCH_2Br$, iPr_2NEt, MeCN, 48%.

(data not shown). The MAPK phosphorylation caused by 3-phosphorylated phosphoinositides lasted much longer than the one caused by EGF. However in a wash-out experiment, the pulse application of PIP_4/AM shortened the duration of MAPK phosphorylation, leading to a transient signaling pattern typical for EGF treatment (Figure S1C and see the quantification in Figure S1D). This is significant because it indicates that the cells are capable of metabolizing PIP_4/AM and deal with increased signaling activity.

Since p42/p44 MAPK phosphorylation levels are a measure of signaling events several steps downstream from PI3K, we tested the phosphorylation status of Akt, which is a more direct downstream target of PI3K/PDK1 signaling (Figure 1A) (Cantley, 2002). Similarly to p42/p44 MAPK phosphorylation experiments, PIP_4/AM induced Akt phosphorylation with remarkable potency (Figure 3B). The highest Akt phosphorylation was induced by PDGF (Figure 3B), which was used as a positive control in these experiments. Similar phosphorylation dynamics were observed for p70S6K (Figure S1E), another direct target of PI3K/PDK1 signaling (Figure 1A) (Cantley, 2002). This demonstrates that membrane-permeant 3-phosphorylated phosphoinositides are able to induce phosphorylation of proteins downstream of PI3K/PDK1, with PIP_4/AM being the most potent derivative.

Given the strong responses of the PIP_4/AM derivative, we wanted to investigate its effects on intracellular signaling in a more global fashion. We measured the phosphorylation state of a large number of cellular proteins using commercial Kinex antibody microarray and Kinetworks multi-immunoblot phosphoprotein-screening platforms (KPSS). Lysates from non-stimulated (control) and PIP_4/AM stimulated HeLa cells were subjected to the Kinex antibody microarray assay, a screen that uses 650 different antibodies to monitor protein expression and phosphorylation levels. Over 40 proteins were found to significantly change phosphorylation levels after PIP_4/AM stimulation (Table S1), many being mediators of PI3K signaling such as Akt, GSK3β, p70S6K, Rac1, Bad, IRS1, FAK, JNK, etc., as well as mediators of MAPK signaling, such as ERK1/2, MEK1/2, MAPKAP2, etc. To confirm these results, we used two different Kinetworks multi-immunoblot assays (KPSS 10.1 and KPSS 11.0), a more accurate western blot-based assay, which uses 30–40 phosphospecific antibodies and 20 lane multichannel blotters. Again, the results showed an increase in the phosphorylation levels of several PI3K signaling mediators such as p70S6K, GSK3β, RSK1/2, JNK, and MAPK signaling members such as ERK1/2 and MEK1/2 (Figures S2A and S2B; lists of all the phosphoproteins tested are shown in Tables S2 and S3). Moreover the phosphorylation pattern induced by PIP_4/AM stimulation resembled that induced by EGF stimulation both qualitatively and quantitatively (Figures S2A and S2B).

To investigate other aspects of PI3K signaling, such as PKC activation, we used KCP-1, a fluorescent sensor that monitors atypical PKC activity in real time (Schleifenbaum et al., 2004), simultaneously with Fura red, a calcium-sensitive sensor. Addition of PIP_4/AM led to an increase in PKC-dependent phosphorylation, but had no effect on intracellular calcium levels (Figure 3E). The lack of calcium response suggested that a non-classic, calcium-independent PKC was triggered by PIP_4/AM, which is exactly the type of PKCs that are known to be activated downstream of PI3K (Toker, 2000). In addition, the PKC sensor used here is predominantly responding to atypical PKC phosphorylation (Schleifenbaum et al., 2004). Interestingly, other 3-phosphorylated phosphoinositides failed to stimulate PKC activity. Possibly, the more powerful trigger of PIP_4/AM is required to allow KCP-1 to respond. From the above data, PIP_4/AM appears to trigger a significant subset of growth factor signaling without the need of growth factor receptor stimulation.

Phosphoinositide Derivatives Induce PH Domain Translocation in Live Cells

Phosphoinositides achieve direct signaling effects through the binding of their head groups to various signaling proteins possessing phosphoinositide binding domain (Di Paolo and De Camilli, 2006). Interaction between 3-phosphorylated phosphoinositides and signaling proteins is often achieved via pleckstrin homology (PH) domains. This interaction regularly results in protein translocation to the plasma membrane (Di Paolo and De Camilli, 2006). We used the GFP-tagged PH domain of Grp1 (Grp1-PH-GFP), a commonly used PtdIns(3,4,5)P_3 sensor (Halet, 2005), and imaged its dynamics after stimulation with PIP_4/AM using live cell confocal microscopy. Stimulation of NRK cells with PIP_4/AM resulted in Grp1-PH-GFP domain translocation to the plasma membrane. Translocation started to be noticeable 3 min after stimulation (Figures 3C and 3D and Movie S1). The translocation was more complete and almost instantaneous when the cell were stimulated with PDGF (Figures 3C and 3D and Movie S2), which was used as a positive control. The same was observed using other PIP_3 sensors such as GFP-tagged PH domain of PDK1 (Figure S3) and Akt (data not shown). Inhibition of endogenous PI3K by wortmannin did not have an effect on PIP_4/AM-induced PH domain translocation while it completely inhibited growth factor-induced translocation (Figure S3). This is in agreement with the aforementioned protein phosphorylation results and suggests that PIP_4/AM is able to translocate relevant PH domain-bearing proteins to the correct

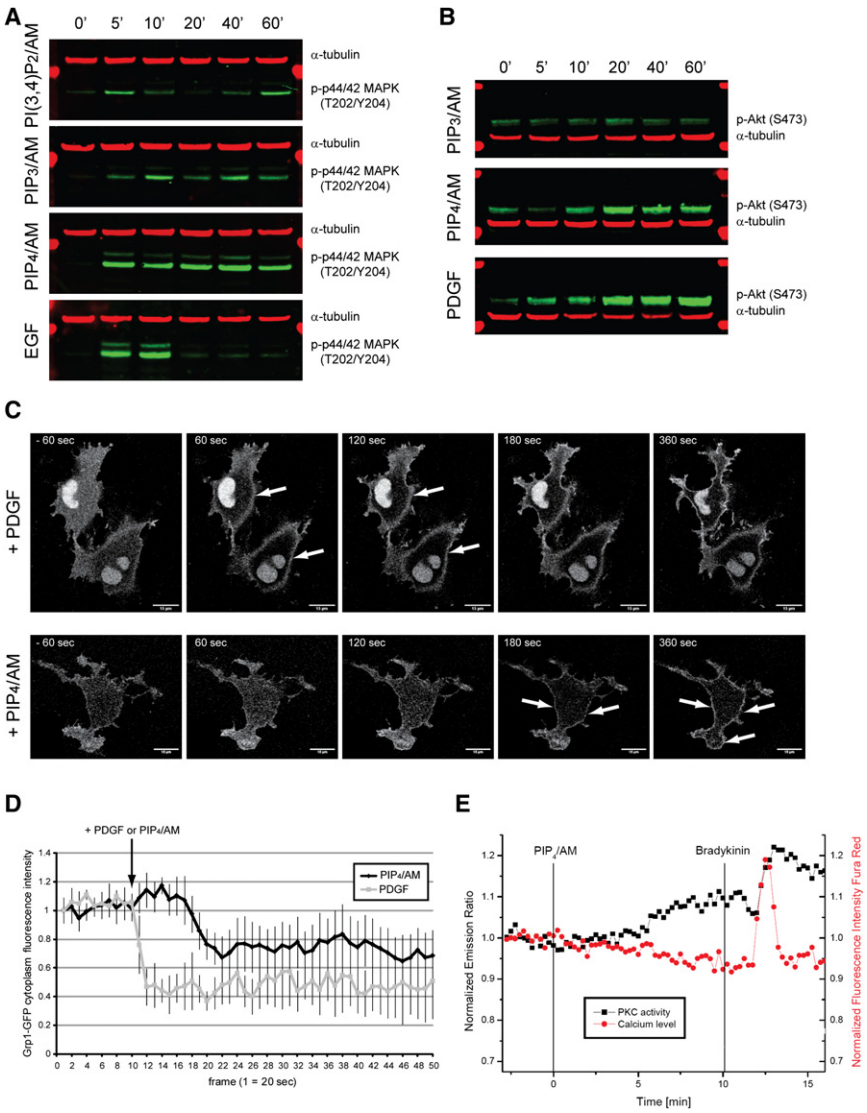

Figure 3. Effects of Membrane-Permeant Phosphoinositide Stimulation on Intracellular Signaling Downstream of PI3K

(A) Time course of p42/44 MAPK phosphorylation after stimulation of HeLa cells with 10 μM $PI(3,4)P_2$/AM, PIP_3/AM, PIP_4/AM, and EGF (100 ng/ml). p42/44 MAPK phosphorylation on residues T202/Y204 is shown in green and α-tubulin control is shown in red. Duration of stimulation in minutes is indicated on the top of the panel.

(B) Time course of Akt phosphorylation after stimulation of NRK cells with PIP_3/AM (10 μM), PIP_4/AM (10 μM), and PDGF (100 ng/ml). Akt phosphorylation on S473 is shown in green and α-tubulin control is shown in red. The time course is shown on top of the panel.

(C) Translocation of the PH-GFP domain of Grp1 (PIP_3 sensor) to the plasma membrane after PDGF (100 ng/ml) or PIP_4/AM (10 μM) treatment of NRK cells. Arrows point to areas where the translocation is the most pronounced. Scale bars, 15 μm.

(D) Quantification of PH-GFP Grp1 domain translocation. Shown is the loss of cytosolic fluorescence as the GFP fusion translocates to the plasma membrane. Error bars represent the SD of the mean of seven cells from three independent experiments.

(E) Multiparameter imaging of events downstream from PI3K. PKC activity is monitored by the FRET-based sensor KCP-1 (black) and calcium levels are measured by the indicator Fura Red (red) (as described in Experimental Procedures).

membrane and activate signaling downstream of PI3K in the presence of PI3K inhibitor. The delay of 3 min in PH domain translocation between growth factor and PIP_4/AM stimulations (Figures 3C and 3D) probably reflects the time needed for the enzymatic reaction required to convert PIP_4/AM to a biologically active compound. We were not able to detect significant PH domain translocation after stimulation with PIP_3/AM, which might explain its lower potency.

To further characterize the onset of PIP_4/AM-induced signaling, we used YFP-tagged p42 MAPK and observed its translocation from the cytosol to the nucleus. In HeLa cells, PIP_4/AM led to YFP-p42 MAPK translocation from the cytosol to the nucleus within several minutes (Figure S4A and Movie S3). Similar to PH domain translocation experiments, YFP-p42 MAPK translocation started 5 min after the stimulation (Figure S4B). EGF stimulation, used as a control, induced almost instantaneous YFP-p42 MAPK translocation (Figures S4A and S4B and Movie S4).

From the present data, it is difficult to determine whether the butyrates of membrane-permeant phosphoinositide derivatives need to be removed for exhibiting biological activity in cells. We therefore incubated the 2-*O*-butyrylated PIP_4 derivative ($BtPIP_4$) and the 2,6-di-O-butyrylated PIP_3 derivative (Bt_2PIP_3) with the two most prominent metabolizing enzymes for PIP_3, PTEN and SHIP2. Both enzymes were very weakly dephosphorylating the compounds (Figure S5), suggesting that the butyrate is required to be removed for rapid dephosphorylation after the washout. In addition, we investigated the recognition of $BtPIP_4$ by the Grb-1 PH domain using surface plasmon resonance experiments. As is shown in Figure S6, only weak binding of the Grp-1 PH domain to $BtPIP_4$-containing vesicles was observed. Again, this implies that the butyrate needs to be removed for the substantial Grp-1 PH domain translocation observed in NRK cells after incubation with PIP_4/AM (Figure 3C).

Regulation of Neurite Formation by Different Phosphoinositides

After investigating the effects of membrane-permeant phosphoinositides **5**, **6**, and **7** in rapidly occurring PI3K-dependent events such as protein phosphorylation and translocation, we were interested in observing more complex, PI3K-regulated physiological processes, such as neurite formation. By using PI3K inhibitors and by overexpressing constitutively active

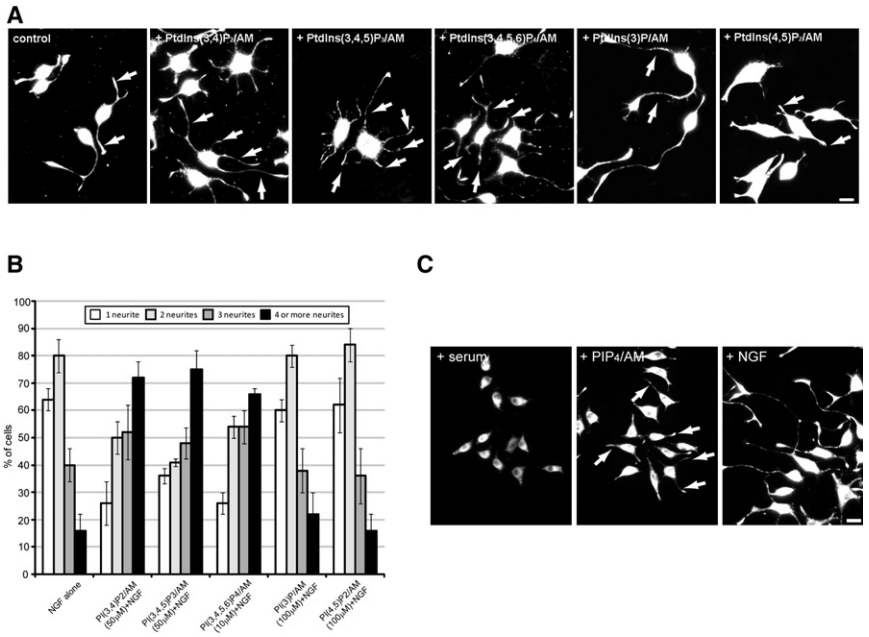

Figure 4. Effects of Membrane-Permeant Phosphoinositides on NGF-Induced Neurite Outgrowth in PC12 Cells

(A) Phenotypes of PC12 cells after 24 hr of stimulation with NGF alone (control) and NGF together with $PI(3,4)P_2$/AM (50 μM), $PI(3,4,5)P_3$/AM (50 μM), PIP_4/AM (10 μM), PI(3)P/AM (100 μM), and $PI(4,5)P_2$/AM (100 μM), respectively. Arrows point to individual neurites. Note that $PI(3,4)P_2$/AM, $PI(3,4,5)P_3$/AM, and PIP_4/AM induced a dramatic increase in the number of neurites per cell, albeit with differences in the required doses, whereas PI(3)P/AM and $PI(4,5)P_2$/AM had no effect on neurite number. Scale bar, 10 μm.

(B) Quantification of the effect of synthetic phosphoinositide derivatives on neurite numbers. Shown are changes in the percentage of cells with 1, 2, 3, and 4 or more neurites per cell in response to treatment with the derivative indicated. Error bars represent SD of the mean of at least 300 cells from two or more independent experiments.

(C) PC12 cell phenotypes after stimulation with serum, PIP_4/AM (10 μM), or NGF (100 ng/ml). Note the appearance of short neurite-like structures (arrows) on PIP_4/AM-stimulated PC12 cells. Scale bar, 10 μm.

PI3K, it has been very well established that neurite outgrowth is a PI3K-dependent process (Kimura et al., 1994; Kobayashi et al., 1997). Furthermore, it has been suggested that the PI3K product, $PtdIns(3,4,5)P_3$, plays a crucial role in neurite initiation (Aoki et al., 2005, 2007), a very early step during neurite outgrowth. However, this has not been directly demonstrated in living cells. To test this directly, we chose PC12 cells stably transfected with human NGF receptor (PC12 6–15), a model cell line for studying early events during neurite outgrowth including neurite initiation (Laketa et al., 2007). This cell line shows rapid responses to NGF and develops neurites on the time scale of hours rather than days, as is the case for standard PC12 cells (Hempstead et al., 1992). When these cells were incubated with 10 μM PIP_4/AM (**6**) in the presence of NGF, they produced dramatically more neurites per cell compared to cells treated with NGF alone (Figures 4A and 4B). While NGF-treated control cells produced an average of two neurites per cell, cells treated with PIP_4/AM (**6**) produced mostly four or more neurites per cell (Figures 3A and 3B). Ten micromoles of PIP_3/AM and $PI(3,4)P_2$/AM had no effect on neurite numbers, again confirming their lower potency (data not shown). However, when the cells were treated with five times higher concentration of PIP_3/AM and $PI(3,4)P_2$/AM, we observed similar effects on neurite number as with PIP_4/AM (Figures 4A and 4B). No effect on the number of neurites per cell was observed when the cells were treated with membrane-permeant $PtdIns(4,5)P_2$ (**4**) or membrane-permeant PtdIns(3)P derivatives (Figures 4A and 4B), demonstrating specificity. This suggests that the number of neurites is under the direct control of 3-O-phosphorylated lipids as products of PI3K.

When cells were incubated with PIP_4/AM in the absence of NGF, a large number of short extensions resembling neurite initiation events were formed within 24 hr (Figure 4C). To be sure that this morphological observation resembles the beginning of a differentiation process we used two additional biochemical indicators. First, suppression of proliferation was measured by the extent of BrdU incorporation into DNA of proliferating cells. Both NGF and PIP_4/AM almost completely abolished BrdU incorporation, indicating suppression of PC12 cell proliferation (Figure S7A). Second, we used a MAPK phosphorylation profile as an indicator of differentiation. It was previously shown that sustained MAPK phosphorylation leads to PC12 cell differentiation, while transient MAPK phosphorylation results in cell proliferation (Marshall, 1995). Both NGF and derivative PIP_4/AM induced a sustained MAPK phosphorylation over 2 hr, which is typical for differentiation processes, while EGF stimulation produced only transient MAPK phosphorylation and failed to trigger neurite initiation (Figure S7B). Taken together, both morphological and biochemical observations indicate that cells undergo a differentiation process in response to the $PtdIns(3,4,5)P_3$-mimicking derivatives such as PIP_4/AM. However, the neurites induced by PIP_4/AM remained short even after 48 hr, suggesting that longitudinal neurite growth depends on additional signals, not triggered by the 3-phosphorylated phosphoinositide derivatives.

DISCUSSION

We have demonstrated, in a comprehensive set of biochemical and live cell assays, that membrane-permeant phosphoinositides are able to stimulate many aspects of PI3K-dependent signaling. Remarkably, the "unnatural" $PtdIns(3,4,5)P_3$ derivative with a phosphate on 6-OH position, PIP_4/AM (**6**), is a much more powerful activator of PI3K signaling than the other 3-O phosphorylated membrane-permeant compounds, also in the presence of PI3K inhibitor. Although our results suggest that endogenous $PtdIns(3,4,5)P_3$ levels are not altered, the precise nature of the biologically active entity produced in cells and the mechanism of action remains to be elucidated. As estimated

by reversed-phase chromatography the hydrophobicity of all membrane-permeant derivatives seems to be very similar. Therefore, large differences in cell entry between the compounds are not expected. Very little is known about structure-activity relationships of phosphoinositides; however, one explanation for higher PIP_4/AM activity comes from closer examination of the PDK1 PH domain crystal structures. The structure shows that the phosphoinositide-binding site of PDK1 is unusually spacious (Komander et al., 2004). In contrast to other PtdIns(3,4,5)P_3-binding PH domains such as those from Akt or Grp1 where the 6-OH position is exposed to the solvent (Lietzke et al., 2000), in the PDK1 PH domain additional binding sites are present around the 6-OH position, which could interact with another phosphate group. In fact, it was demonstrated that PDK1 binds 6-OH phosphorylated inositol phosphates, such as Ins(1,3,4,5,6)P_5 and $InsP_6$, with submicromolar affinity, whereas binding to inositol phosphates without the phosphate on the 6-OH position, such as Ins(1,4,5)P_3, is virtually undetectable (Komander et al., 2004). It is therefore possible that PIP_4/AM-derived phosphoinositides, by having an additional phosphate on 6-OH position, may bind to PDK1 with higher affinity than those from the similar compound PIP_3/AM and consequently induce the PI3K signaling pathways more effectively. Alternatively, the higher activity could be assigned to a slower metabolism of the biologically active product in cells by endogenous phosphatases and/or the lack of butyrate hydrolysis required in the 6-OH position. Finally, we cannot entirely exclude that PtdIns(3,4,5,6)P_4 occurs in living cells as a putative messenger lipid and that its very low abundance has prevented detection so far. Despite our current lack of understanding of the precise mode of action, PIP_4/AM will likely become an attractive tool to study growth factor signaling in the future, especially considering its comparably facile synthesis and potency. A technical problem to be considered in this respect is the low shelf-life of about six months for this type of compound.

Application of PI(3,4)P_2/AM, PIP_3/AM, and PIP_4/AM together with NGF induced a significant increase in the number of neurites per cell, which is consistent with their role in neurite initiation discussed in the literature. Aoki et al. (2005, 2007), using FRET based PtdIns(3,4,5)P_3 sensors, showed that local accumulation of PtdIns(3,4,5)P_3 initiates neurite protrusion at the plasma membrane and constructed a model for neurite initiation in silico based on regulation of PIP_3 levels. Furthermore, Fivaz et al. (2008) have shown that the local PI3K-HRas-positive feedback loop is instrumental for breaking the initial neuronal symmetry and for neurite initiation. These studies failed to directly test the hypothesis that more PtdIns(3,4,5)P_3 will lead to more neurites in vivo. Our results are thus complementing these studies by showing that application of membrane-permeant PI3K products leads to a dramatic increase in the number of neurites per cell. Also, we provide a direct demonstration of the involvement of these phosphoinositides in neurite initiation.

Together with the biochemical and live cell data on signaling network activation downstream of PI3K/PDK1, we show that membrane-permeant phosphoinositide derivatives are useful to study both immediate PI3K-dependent events such as protein phosphorylation and translocation, as well as complex PI3K-dependent cellular processes, which take many hours to develop, such as neurite outgrowth.

SIGNIFICANCE

In order to facilitate the investigation of PI3K signaling and the function of the various phosphoinositides, methods are needed that artificially, acutely, but nondisruptively, increase the concentration of a specific phospholipid. This work demonstrates that membrane-permeable phosphoinositide derivatives are suitable for rapidly activating intracellular signaling pathways downstream of PI3K. This makes them important tools to investigate the contribution of phosphoinositide signaling in living cells. We have synthesized a phosphoinositide analog with a phosphate on the 6-OH position, which showed remarkable potency in activating PI3K-dependent signaling. Although phosphoinositides with a phosphate on this position have not been detected in vivo, we cannot entirely exclude that PtdIns(3,4,5,6)P_4 occurs in living cells as a putative messenger lipid that escaped detection due to its very low abundance. In addition, we show that membrane-permeant phosphoinositides are able to modulate complex PI3K-dependent processes such as neurite initiation and outgrowth. Previous work has suggested that the PI3K product PtdIns(3,4,5)P_3 plays a crucial role in neurite initiation but the hypothesis that more PtdIns(3,4,5)P_3 will lead to more neurites in vivo was never directly tested. The increase in the number of neurites per cell after application of membrane-permeant PI3K products is complementing earlier neurite initiation studies from other labs and provides a direct demonstration of the involvement of these phosphoinositides in neurite initiation. In the future, membrane-permeant derivatives that are limited in their metabolism or photoactivatable varieties might pave the way for even more exciting possibilities.

EXPERIMENTAL PROCEDURES

Cell Lines and Antibodies

PC12 6–15 cells (stably transfected with NGF receptor TrkA) were a gift from D. Martin Zanca (University of Salamanca). NRK cells were a gift from J. Ellenberg (European Molecular Biology Laboratory). U2OS cells were a gift from A. Dinarina (Spanish National Cancer Research Centre). HeLa CCL-2 cells were purchased from LGC Promochem GmbH. Anti-phosphoERK1/2 (T202/Y204), anti-phosphoAkt (S473), and anti-phosphop70S6K (T389) were purchased from Cell Signaling Technology. Anti-α-tubulin antibody was obtained from NeoMarkers. Secondary antibodies for western blots were goat anti-rabbit IRDye 800CW (Rockland Immunologicals) and goat anti-mouse Alexa-680 (Molecular Probes).

Imaging of PH Domain and MAPK Translocation

NRK or HeLa cells were grown on 35 mm glass-bottom dishes (MatTek). The NRK were transfected with GFP-tagged PH domain of Grp1 while HeLa cells were transfected with YFP-tagged ERK1 using Fugene6 (Roche) according to the manufacturer's protocol. After the 12–16 hr starvation in serum-free DMEM, the cells were imaged using a Leica SP2 AOBS confocal microscope with a 63× oil objective in PH domain translocation experiments or using a Leica AF6000 LX widefield microscope with a 60× glycerol objective for studying MAPK translocation.

Ca^{2+} and PKC Activity Imaging

HeLa CCL-2 cells (LGC Promochem GmbH) were transfected with KCP-1 using Fugene6 (Roche). After 12 hr the cells were incubated for 30 min with 15 μM Fura Red/AM (Molecular Probes) and imaged using a Leica SP2 AOBS confocal microscope with a 63× oil immersion objective (Leica). FRET

measurements with KCP-1 were carried out as previously described (Schleifenbaum et al., 2004).

Neurite Outgrowth Assay

Neurite outgrowth assay was performed as previously described (Laketa et al., 2007; also available in the Supplemental Experimental Procedures).

Western Blot Assay

HeLa or NRK cells were grown in a 6 well dish in DMEM and 10% fetal calf serum. After 12–16 hr starvation in serum-free DMEM, the cells were treated with EGF (100 ng/ml) and PDGF (100 ng/ml) (Sigma-Aldrich) or with various concentrations of membrane-permeant phosphoinositide derivatives **4**–**7**. Obtained lysates were analyzed using standard western blot protocols. Antibody signal detection was performed with an Odyssey Infrared Imaging System (LI-Cor Biosystems).

Protein Phosphorylation Screens

Detergent-solubilized extracts from non-stimulated (control) and PIP_4/AM (10 μM)-stimulated HeLa cells were subjected to Kinex antibody microarray screen. Also, extracts from non-stimulated (control), PIP_4/AM (10 μM)-, and EGF (100 ng/ml)-stimulated HeLa cells were subjected to KPSS 10.1 and KPSS 11.0 as described on the Kinexus Bioinformatics Corp. website (http://www.kinexus.ca). Kinex antibody microarray screen uses a panel of 650 antibodies to track the differential binding of dye-labeled proteins in lysates prepared from stimulated versus non-stimulated cells. This screen was performed twice. KPSS 10.1 and KPSS 11.0 screens use panels of 30–40 highly validated commercial phosphosite-specific antibodies and 20 lane multichannel blotters. The intensity of the ECL signals for the target protein bands on the Kinetworks immunoblots were quantified with a FluorS Max Multi-Imager and Quantity One software (Bio-Rad).

The extended description of the experimental procedures and chemical materials is available in the Supplemental Experimental Procedures.

SUPPLEMENTAL DATA

Supplemental Data include Supplemental Experimental Procedures, seven figures, three tables, and four movies and can be found with this article online at http://www.cell.com/chemistry-biology/supplemental/S1074-5521(09)00332-9.

ACKNOWLEDGMENTS

We thank H. Stichnoth for cultured cells and J. Gross (University of Heidelberg) for high resolution mass determination. Funding was provided by the VW foundation (I/81 597) and the Helmholtz Initiative for Systems Biology (SBCancer) to C.S. R.P. is supported by a grant from the German Federal Ministry of Education and Research within the framework of NGFN2 SMP Cell (01GR0423).

Received: July 6, 2009
Revised: October 6, 2009
Accepted: October 7, 2009
Published: November 24, 2009

REFERENCES

Aoki, K., Nakamura, T., Fujikawa, K., and Matsuda, M. (2005). Local phosphatidylinositol 3,4,5-trisphosphate accumulation recruits Vav2 and Vav3 to activate Rac1/Cdc42 and initiate neurite outgrowth in nerve growth factor-stimulated PC12 cells. Mol. Biol. Cell *16*, 2207–2217.

Aoki, K., Nakamura, T., Inoue, T., Meyer, T., and Matsuda, M. (2007). An essential role for the SHIP2-dependent negative feedback loop in neuritogenesis of nerve growth factor-stimulated PC12 cells. J. Cell Biol. *177*, 817–827.

Bartsch, M., Zorn-Kruppa, M., Kuhl, N., Genieser, H.G., Schwede, F., and Jastorff, B. (2003). Bioactivatable, membrane-permeant analogs of cyclic nucleotides as biological tools for growth control of C6 glioma cells. Biol. Chem. *384*, 1321–1326.

Cantley, L.C. (2002). The phosphoinositide 3-kinase pathway. Science *296*, 1655–1657.

Cuevas, B.D., Abell, A.N., and Johnson, G.L. (2007). Role of mitogen-activated protein kinase kinase kinases in signal integration. Oncogene *26*, 3159–3171.

Di Paolo, G., and De Camilli, P. (2006). Phosphoinositides in cell regulation and membrane dynamics. Nature *443*, 651–657.

Dinkel, C., Moody, M., Traynor-Kaplan, A., and Schultz, C. (2001). Membrane-permeant 3-OH-phosphorylated phosphoinositide derivatives. Angew. Chem. Int. Ed. Engl. *40*, 3004–3008.

Fivaz, M., Bandara, S., Inoue, T., and Meyer, T. (2008). Robust neuronal symmetry breaking by Ras-triggered local positive feedback. Curr. Biol. *18*, 44–50.

Halet, G. (2005). Imaging phosphoinositide dynamics using GFP-tagged protein domains. Biol. Cell *97*, 501–518.

Hempstead, B.L., Rabin, S.J., Kaplan, L., Reid, S., Parada, L.F., and Kaplan, D.R. (1992). Overexpression of the trk tyrosine kinase rapidly accelerates nerve growth factor-induced differentiation. Neuron *9*, 883–896.

Jiang, T., Sweeney, G., Rudolf, M.T., Klip, A., Traynor-Kaplan, A., and Tsien, R.Y. (1998). Membrane-permeant esters of phosphatidylinositol 3,4,5-trisphosphate. J. Biol. Chem. *273*, 11017–11024.

Kimura, K., Hattori, S., Kabuyama, Y., Shizawa, Y., Takayanagi, J., Nakamura, S., Toki, S., Matsuda, Y., Onodera, K., and Fukui, Y. (1994). Neurite outgrowth of PC12 cells is suppressed by wortmannin, a specific inhibitor of phosphatidylinositol 3-kinase. J. Biol. Chem. *269*, 18961–18967.

Kobayashi, M., Nagata, S., Kita, Y., Nakatsu, N., Ihara, S., Kaibuchi, K., Kuroda, S., Ui, M., Iba, H., Konishi, H., et al. (1997). Expression of a constitutively active phosphatidylinositol 3-kinase induces process formation in rat PC12 cells. Use of Cre/loxP recombination system. J. Biol. Chem. *272*, 16089–16092.

Komander, D., Fairservice, A., Deak, M., Kular, G.S., Prescott, A.R., Peter Downes, C., Safrany, S.T., Alessi, D.R., and van Aalten, D.M. (2004). Structural insights into the regulation of PDK1 by phosphoinositides and inositol phosphates. EMBO J. *23*, 3918–3928.

Laketa, V., Simpson, J.C., Bechtel, S., Wiemann, S., and Pepperkok, R. (2007). High-content microscopy identifies new neurite outgrowth regulators. Mol. Biol. Cell *18*, 242–252.

Lietzke, S.E., Bose, S., Cronin, T., Klarlund, J., Chawla, A., Czech, M.P., and Lambright, D.G. (2000). Structural basis of 3-phosphoinositide recognition by pleckstrin homology domains. Mol. Cell *6*, 385–394.

Marshall, C.J. (1995). Specificity of receptor tyrosine kinase signaling: transient versus sustained extracellular signal-regulated kinase activation. Cell *80*, 179–185.

Ozaki, S., DeWald, D.B., Shope, J.C., Chen, J., and Prestwich, G.D. (2000). Intracellular delivery of phosphoinositides and inositol phosphates using polyamine carriers. Proc. Natl. Acad. Sci. USA *97*, 11286–11291.

Schleifenbaum, A., Stier, G., Gasch, A., Sattler, M., and Schultz, C. (2004). Genetically encoded FRET probe for PKC activity based on pleckstrin. J. Am. Chem. Soc. *126*, 11786–11787.

Schultz, C. (2003). Prodrugs of biologically active phosphate esters. Bioorg. Med. Chem. *11*, 885–898.

Suh, B.C., Inoue, T., Meyer, T., and Hille, B. (2006). Rapid chemically induced changes of PtdIns(4,5)P2 gate KCNQ ion channels. Science *314*, 1454–1457.

Toker, A. (2000). Protein kinases as mediators of phosphoinositide 3-kinase signaling. Mol. Pharmacol. *57*, 652–658.

Vajanaphanich, M., Schultz, C., Rudolf, M.T., Wasserman, M., Enyedi, P., Craxton, A., Shears, S.B., Tsien, R.Y., Barrett, K.E., and Traynor-Kaplan, A. (1994). Long-term uncoupling of chloride secretion from intracellular calcium levels by Ins(3,4,5,6)P4. Nature *371*, 711–714.

